# Supplementary Materials

## Reactive pulsed laser deposition of clustered-type $MoS_x$ ($x$~2, 3, and 4) films and their solid lubricant properties at low temperature

V. Fominski [1,*], M. Demin[2], V. Nevolin[1], D. Fominski[1], R. Romanov [1], M. Gritskevich[1], N. Smirnov[3]

[1]National Research Nuclear University MEPhI (Moscow Engineering Physics Institute), Moscow, Kashirskoe sh., 31, Russia, 115409

[2]Russia Immanuel Kant Baltic Federal University, Kaliningrad, A. Nevskogo str. 14, Russia, 236016

[3]Mechanical Engineering Research Institute of the Russian Academy of Sciences, Moscow, Bardina Ulitsa 4, Russia, 119334

# Local atomic structures/cluster unites of amorphous $MoS_x$ materials with varied S content

## $MoS_{x\sim2}$

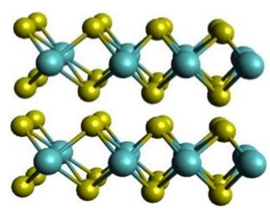

Lamellar/layered-type structure

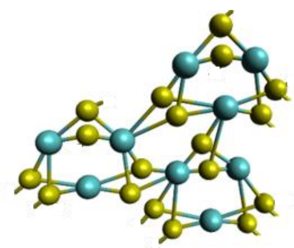

$Mo_3$-S ($Mo_3S_6$) cluster units

## $MoS_{x\sim3}$

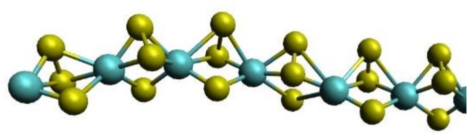

Linear chain of Mo-$S_3$ ($MoS_3$) cluster nits

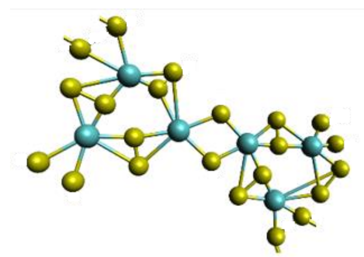

$Mo_3$-S ($Mo_3S_9$) cluster units

## $MoS_{x\sim4}$

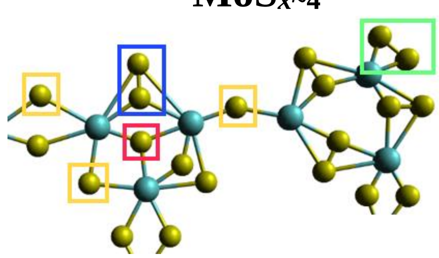

Polymer-like chain consisted of $Mo_3S_{12}$ and $Mo_3S_{13}$ cluster units

**Figure S1.** Possible local structures/atomic packings in amorphous $MoS_x$ coatings with $x$~2, 3, and 4 (Mo atoms – blue, S atoms – yellow). Different types of S ligands that may present in polymerized amorphous $MoS_x$ structures are indicated for $Mo_3S_{12}$ and $Mo_3S_{13}$ cluster unites in colored squares: green, terminal $S_2^{2-}$; red, apical $S^{2-}$; blue, bridging $S_2^{2-}$; yellow, unsaturated $S^{2-}$.

**Tribometer for friction testing of thin-film coatings by pin-on-dis method at various conditions**

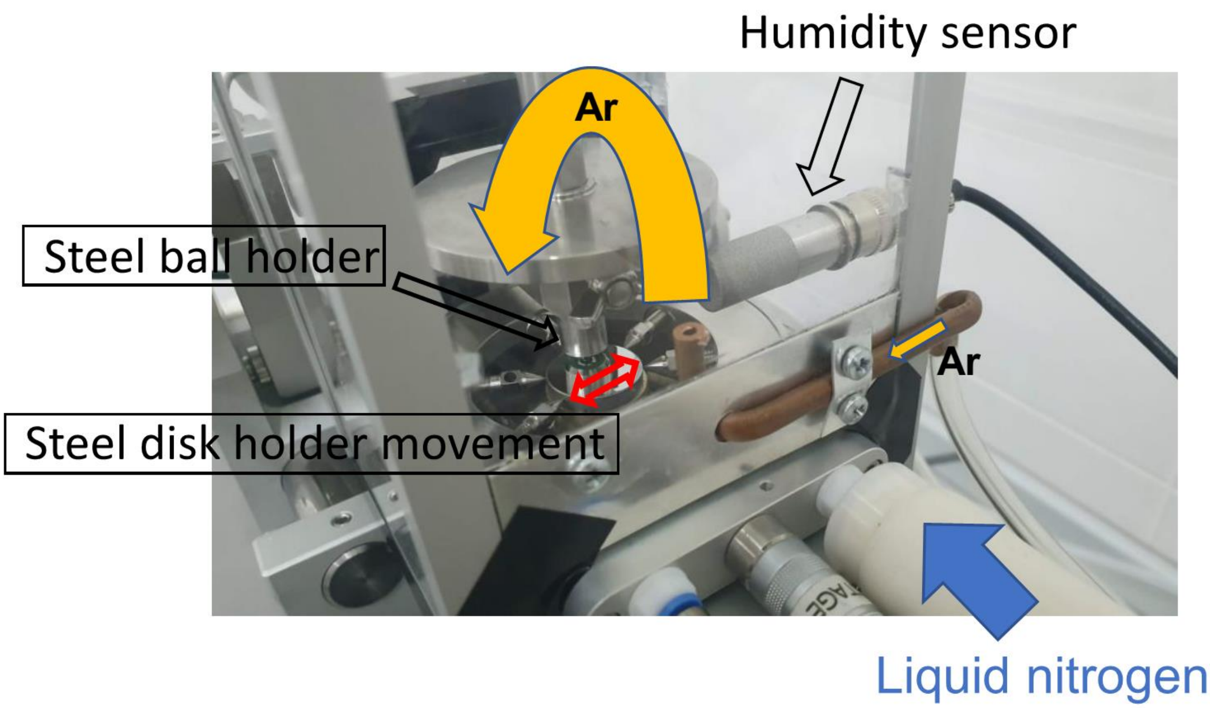


**Figure S2.** Anton Paar TRB3 tribometer modified by the authors for friction testing of $MoS_x$ thin-film coatings at low temperatures.

## Composition and surface distribution of elements for $MoS_x$ thin-film coatings obtained by RPLD

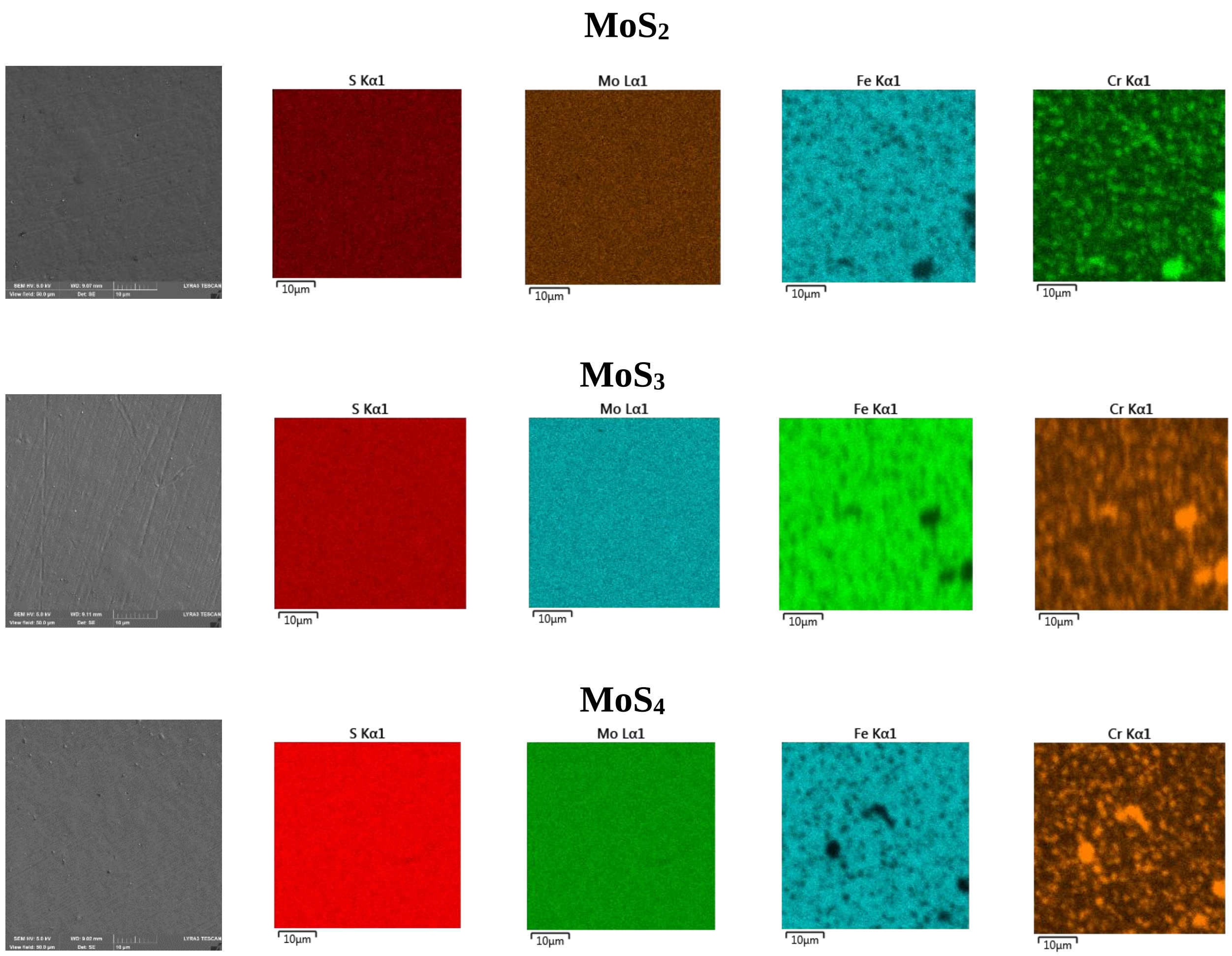


**Figure S3.** Chemical mapping of S, Mo, Fe, and Cr over the surface of different samples obtained by RPLD of $MoS_x$ coatings on the polished steel substrates.

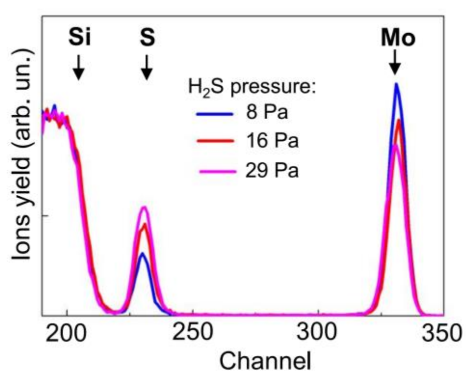


**Figure S4.** RBS spectra for thin $MoS_x$ films obtained by RPLD on Si substrates at different pressures of $H_2S$ gas.

## Monitoring of laser-initiated ion fluxes bombarded the $MoS_x$ coating during RPLD at different pressures of $H_2S$ gas

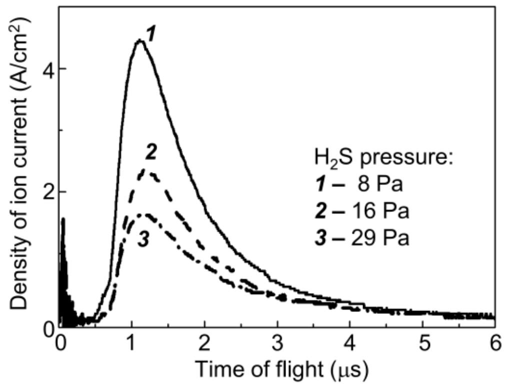


**Figure S5.** Time-of-flight (TOF) signals of ion pulses detected by an ion probe during the pulsed laser ablation of a Mo target at different pressures of $H_2S$ gas.

## Structural study of $MoS_4$ film obtained by RPLD

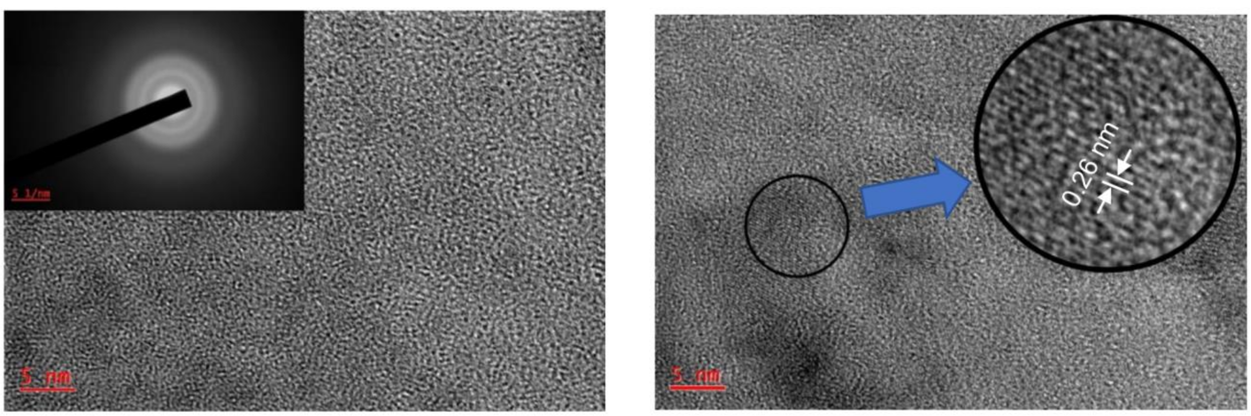


(**a**) (**b**)

**Figure S6.** High resolution TEM and SAED patterns for thin $MoS_4$ film obtained by RPLD. The time of *in situ* electron beam irradiation of the film in the microscope was (**a)** 2 and (**b**) 10 minutes. The e-beam irradiation caused the local modification/crystallization of the film. Lattice spacing in the e-beam induced nanophase was ~0.26 nm. The nature of this nanophase has not been established. It can be assumed that the electron irradiation caused the desorption of sulfur atoms and, as a result, the local formation of the $Mo_2S_3$ nanocrystals in the amorphous $MoS_x$ matrix. The high resolution TEM image of this compound clearly showed the lattice spacing of 0.255 nm [1].

## Distribution of wear along the tracks for $MoS_2$, $MoS_3$, and $MoS_4$ coatings

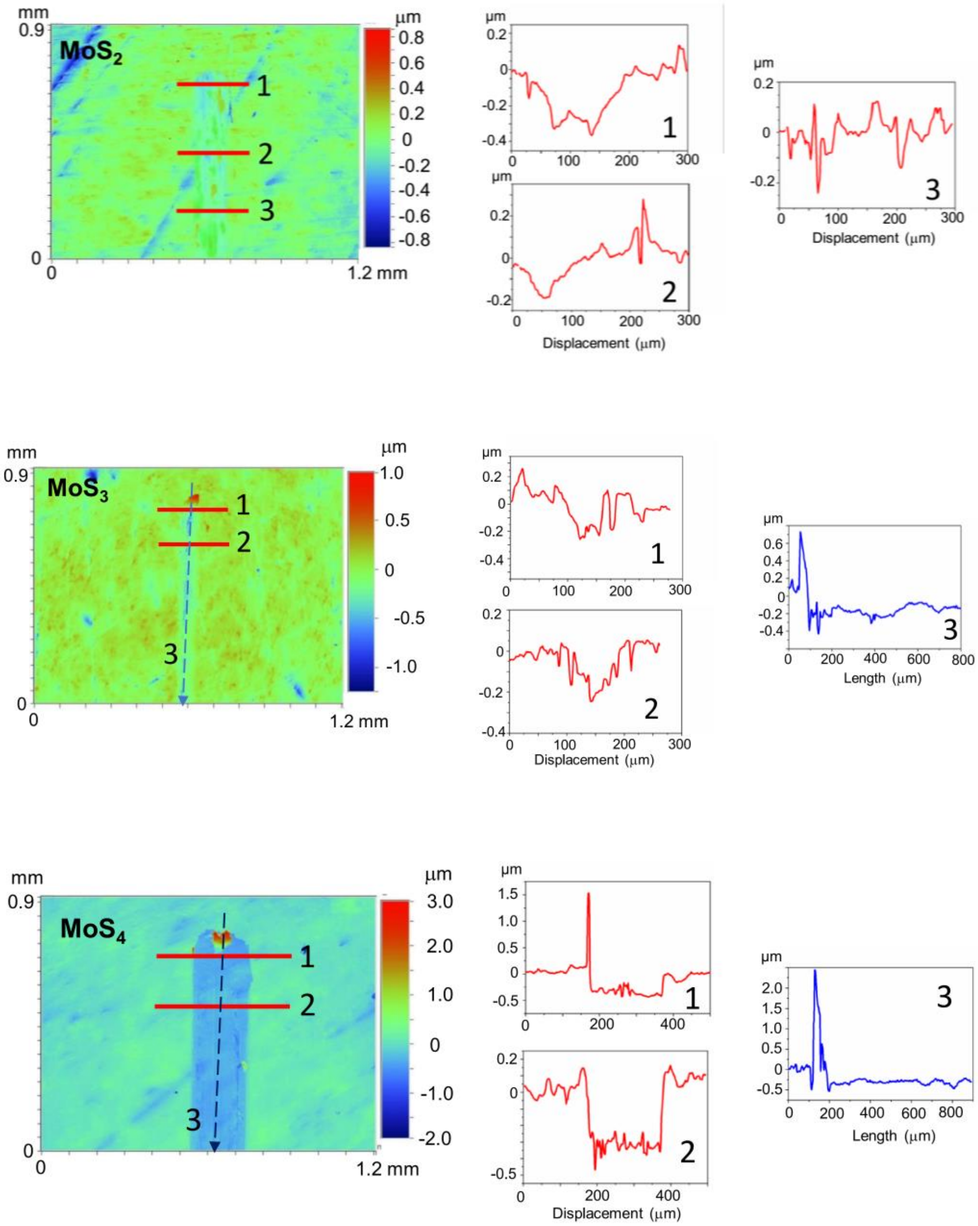


**Figure S7.** 2D images and profiles of the wear scar edge for the different $MoS_x$ coatings measured after tribo-testing at -100°C in an oxidizing environment. Red lines show the cross sections of wear scars at indicated places; blue lines show the depths of the tracks alone the direction of ball sliding. For the $MoS_2$ coating, the profilometry studies revealed the uneven wear along the entire track, therefore, sufficiently accurate profiling along the track could not be done.

# Wear of RPLD $MoS_x$ coatings caused by tribotesting at -100°C

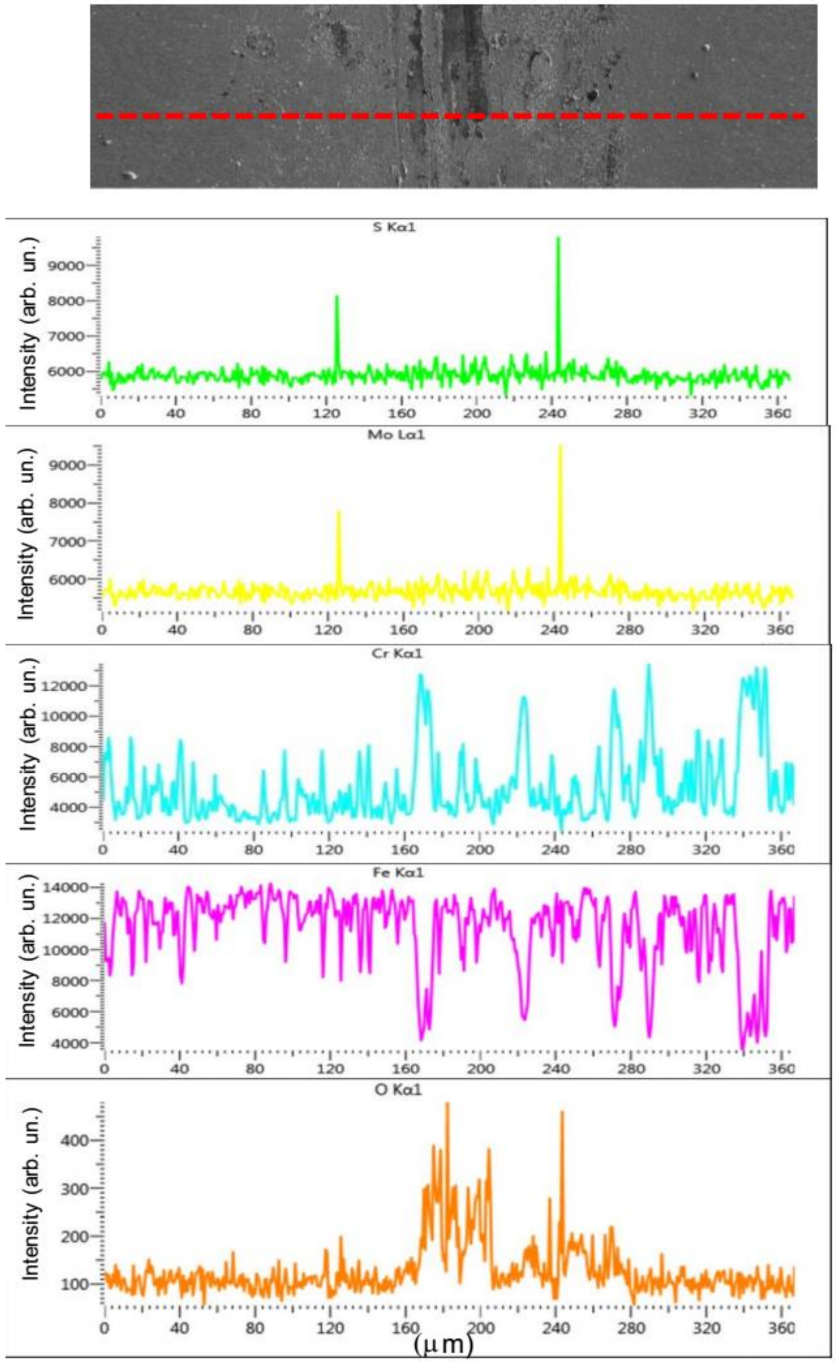


**Figure S8**. Distribution of elements (Mo, S, Fe, Cr, and O) across the central part of the wear track on the $MoS_2$ coating after tribo-testing at -100°C in an oxidizing environment.

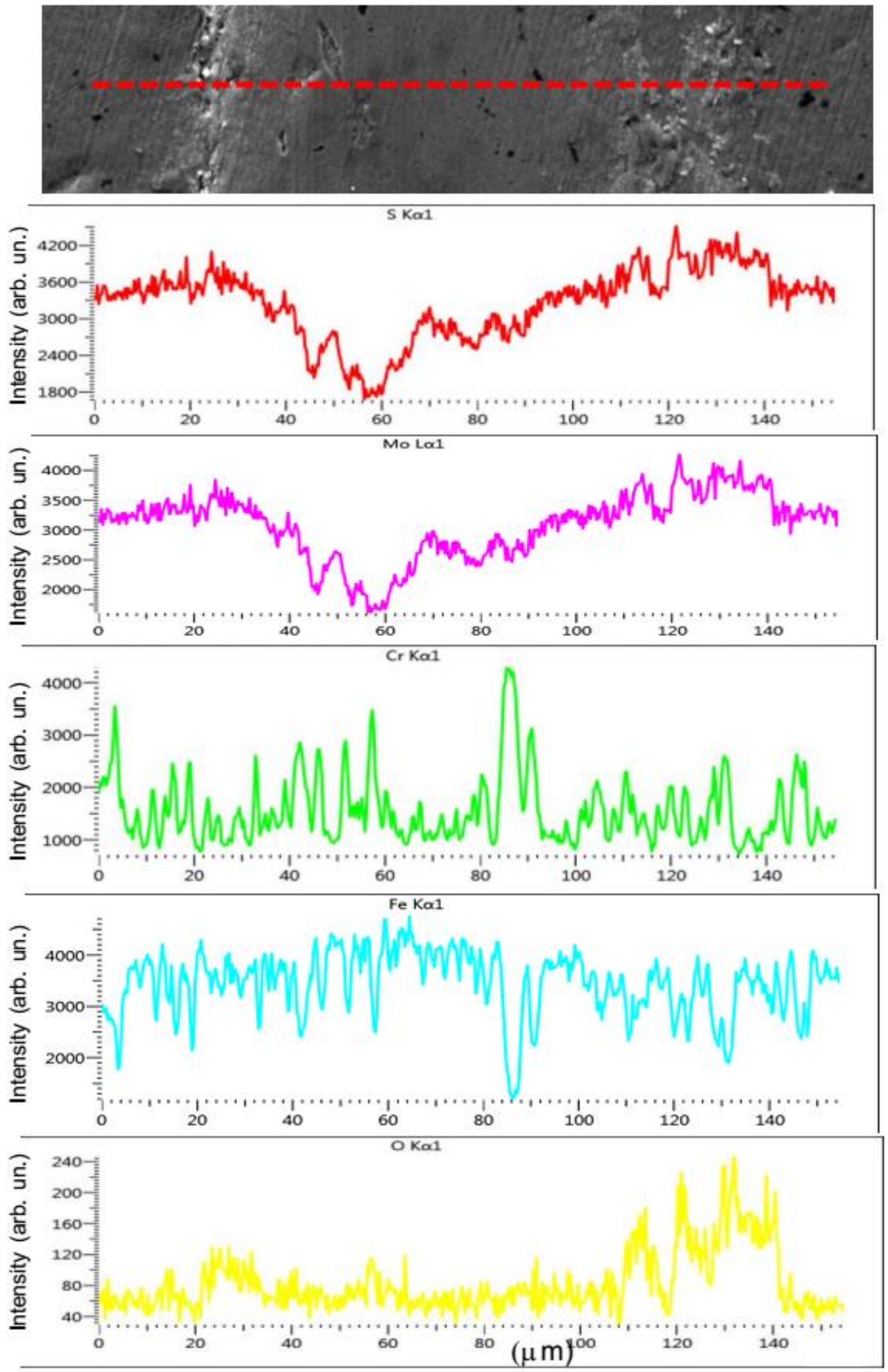


**Figure S9**. Distribution of elements (Mo, S, Fe, Cr, and O) across the central part of the wear track on the $MoS_3$ coating after tribo-testing at -100°C in an oxidizing environment.

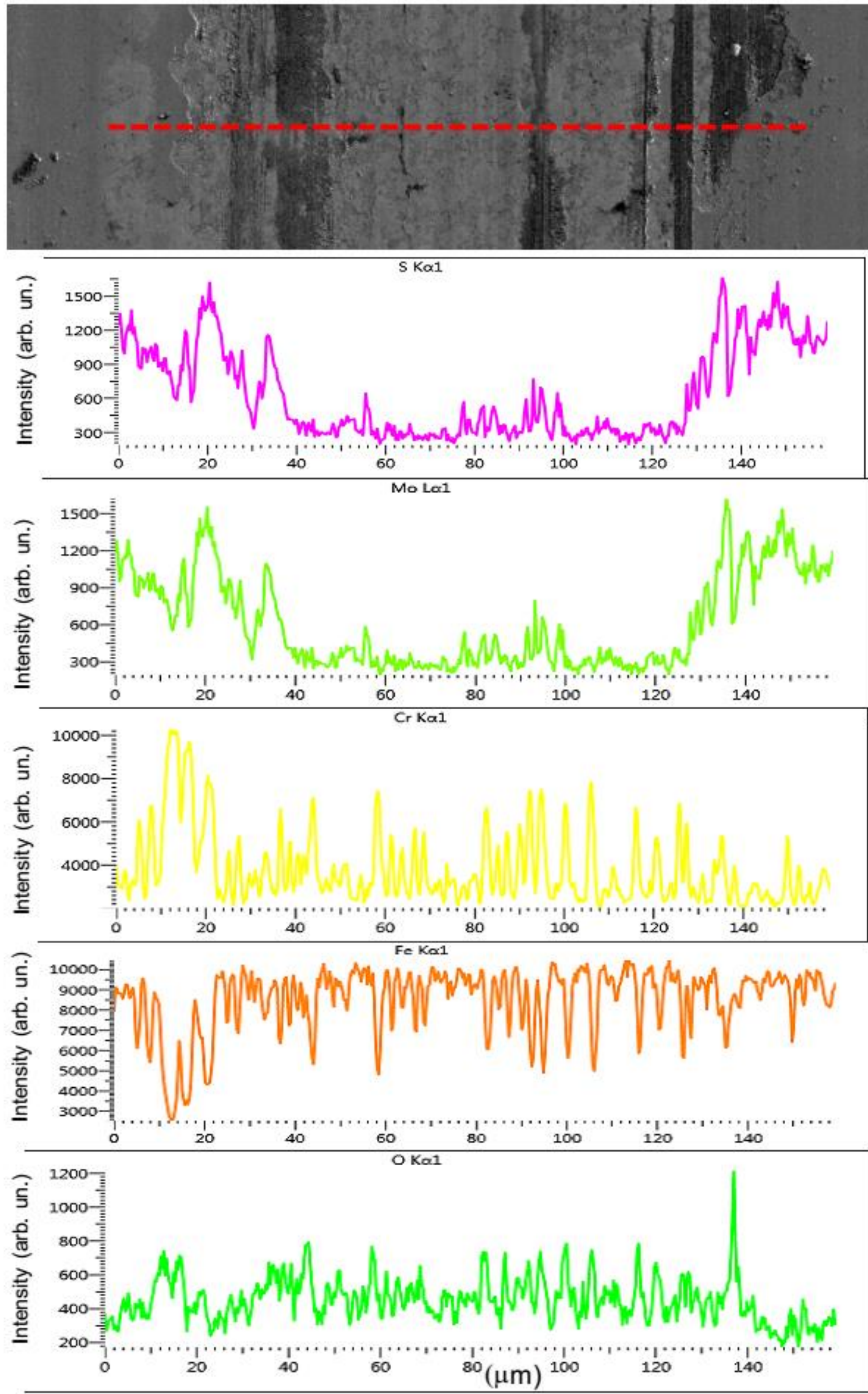


**Figure S10.** Distribution of elements (Mo, S, Fe, Cr, and O) across the central part of the wear track on the $MoS_4$ coating after tribo-testing at -100°C in an oxidizing environment.

# Tribological properties of RPLD MoS$_x$ coatings at 22°C

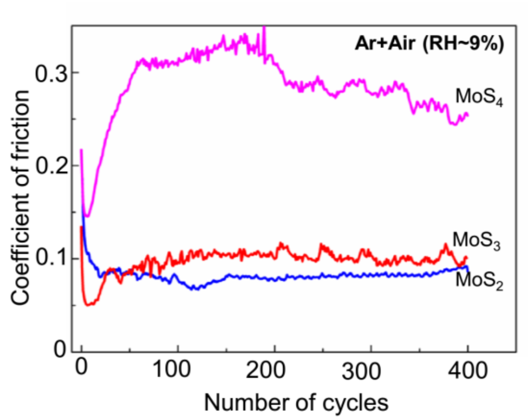


**Figure S11**. Friction curves of tests conducted at 22°C for different RPLD MoS$_x$ coatings in an argon–air mixture (RH~9%).

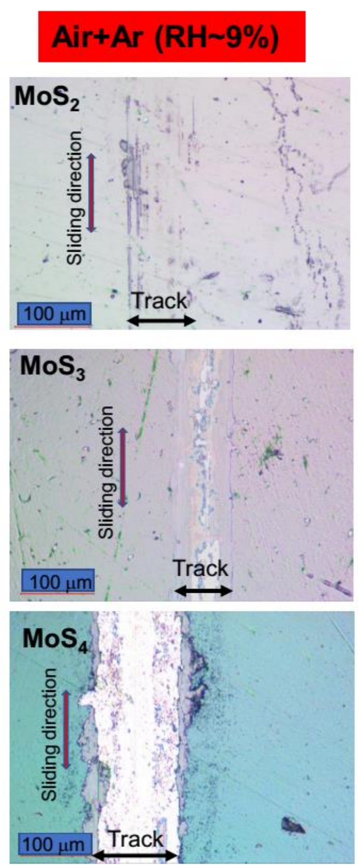


**Figure S12.** Optical images of the wear tracks for different MoS$_x$ coatings after tribo-testing at 22°C in an argon–air mixture (RH~9%).

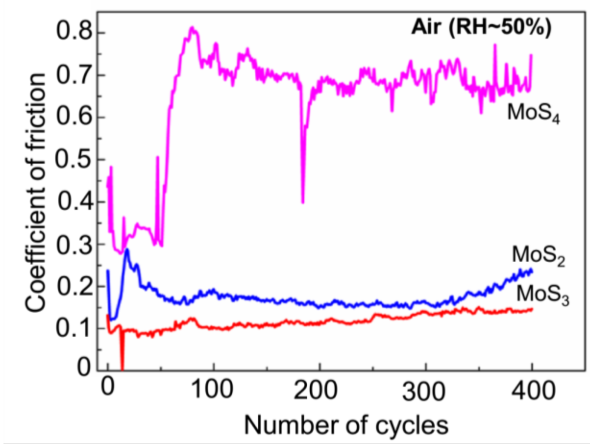


**Figure S13.** Friction curves of tests conducted at 22°C for different RPLD $MoS_x$ coatings in air (RH~50%).

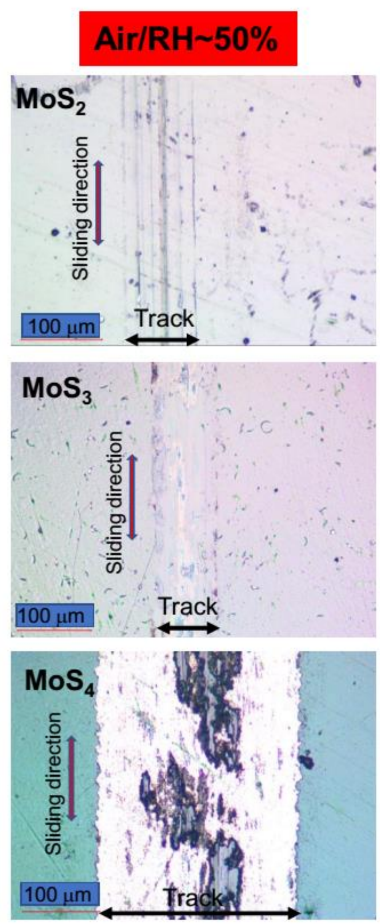


**Figure S14.** Optical images of the wear tracks for different $MoS_x$ coatings after tribo-testing at 22°C in air (RH~50%).

## Reference

1. X. Zhou, W. Zhao, J. Pan, Y. Fang, F. Wang, F. Huang, Urchin-like $Mo_2S_3$ prepared via a molten salt assisted method for efficient hydrogen evolution, Chem. Commun. 2018, 54, 12714.